

# MASS TRANSFER THROUGH LAMINAR BOUNDARY LAYERS— 2. AUXILIARY FUNCTIONS FOR THE VELOCITY BOUNDARY LAYER

D. B. SPALDING and H. L. EVANS

Imperial College of Science and Technology, London, S.W.7

(Received April 1960)

**Abstract**—The auxiliary functions needed in using the method of Paper 1 of the series are presented as graphs and tables (Tables 7 and 8, Figs. 4 and 5). They have been deduced by interpolation from a large number of exact solutions obtained by other authors; these solutions are surveyed in the present paper. It is shown that further exact solutions are needed.

**Résumé**—Les fonctions auxiliaires nécessaires dans l'application de la méthode exposée dans la partie 1 de cet article sont présentées sous forme de graphiques et de tableaux (Tableaux 7 et 8, Figures 4 et 5). Elles ont été obtenues par l'interpolation d'un grand nombre de solutions exactes données par d'autres auteurs; ces solutions sont résumées dans cet article. Il est montré que d'autres solutions exactes seront nécessaires.

**Zusammenfassung**—In der ersten Arbeit dieser Reihe war eine Methode angegeben, deren Anwendung Hilfsfunktionen erfordert. Diese Hilfsfunktionen sind hier als Diagramme und Tabellen (Fig. 4 und 5, Tab. 7 und 8) mitgeteilt. Sie wurden durch Interpolation aus einer grossen Zahl von exakten Lösungen anderer Autoren erhalten. Die kritische Beurteilung dieser Lösungen in der vorliegenden Arbeit zeigt, dass weitere exakte Lösungen notwendig sind.

**Аннотация**—В виде графиков и таблиц (табл. 7 и 8, фиг. 4 и 5) представлены вспомогательные функции, необходимые для расчётов по методу, изложенному в статье 1 настоящей серии работ. Вспомогательные функции были получены интерполяцией большого числа точных решений других авторов; в статье даётся обзор этих решений. Показано, что необходимы новые точные решения.

## NOTATION\*

$C$ , a constant (various) (see equation (9));  
 $c_f$ , drag coefficient (—) (see Section 2.1);  
 $Eu$ , Euler number (—) (see equation (17));  
 $f$ , dimensionless stream function (—) (see equation (1));  
 $f_0$ , dimensionless measure of mass transfer rate (—) (see equation (8));  
 $f_0''$ , dimensionless shear stress at wall (—) (see equations (3) and (7));  
 $F_2$ , measure of rate of growth of momentum thickness (—) (see equation (5));  
 $g_0$ , constant in Newton's Second Law ( $\text{lb}_m\text{ft}/\text{lb}_f\text{h}^2$ ) (see Section 2.1);

$H_{12}$ , ratio of displacement thickness to momentum thickness (—) (see equation (6));  
 $H_{24}$ , ratio of displacement thickness to shear thickness (—) (see equation (7));  
 $m$ , alternative symbol for Euler number,  $Eu$  (—);  
 $n$ , a constant (—) (see equations (9) and (10));  
 $u_G$ , velocity of main stream outside boundary layer (ft/h);  
 $v_S$ , velocity component through wall in direction of fluid (N.B. Mass transfer =  $v_S$  times fluid density adjacent wall) (ft/h);  
 $x$ , distance along wall measured in stream direction (ft);

\* Typical units of measurement are indicated in brackets. (—) signifies dimensionless.

$\beta$ ,	a constant (—) (see equation (10));
$\delta_1$ ,	displacement thickness (ft) (see Paper 1);
$\delta_2$ ,	momentum thickness (ft) (see Paper 1);
$\delta_4$ ,	shear thickness (ft) (see Paper 1);
$\eta$ ,	dimensionless space co-ordinate (—) (see equation (1));
$\nu$ ,	kinematic viscosity of fluid (ft <sup>2</sup> /h);
$\rho$ ,	fluid density (lb <sub>m</sub> /ft <sup>3</sup> );
$\tau_s$ ,	shear stress at wall (lb <sub>f</sub> /ft <sup>2</sup> );
$\phi$ ,	$f\sqrt{-1}$ (—) (see equation (27));
$\chi$ ,	$\eta\sqrt{-1}$ (—) (see equation (28)).

## 1. INTRODUCTION

### 1.1. Purpose of paper

THIS paper is the second of a series dealing with the prediction of mass transfer rates through laminar boundary layers. In the first of these papers (Spalding [1]), a method was presented for calculating the thickness of the velocity boundary layer in the presence of mass transfer. That method pre-supposed the availability of certain functions obtained from the "similar" solutions of the laminar boundary-layer equations.

The main purpose of the present paper is to supply these functions in the form of graphs and tables suitable for practical use. Their method of construction will be explained.

It will appear that the range covered by the functions presented is not as great as is desirable, a restriction that can only be removed by obtaining new solutions to the fundamental equation. A minor purpose of the present paper is therefore to survey the extent to which the velocity of the laminar boundary layer has so far been explored; it will appear that considerable tracts of uncharted territory still remain.

### 1.2. The mathematical problem

In Paper 1 of this series it has been shown that the equation to which the solutions are required is:

$$\frac{d^3 f}{d\eta^3} + \frac{f d^2 f}{d\eta^2} + \beta \left\{ 1 - \left( \frac{df}{d\eta} \right)^2 \right\} = 0 \quad (1)$$

with boundary conditions:

$$\left. \begin{aligned} \eta = 0 : \quad \frac{df}{d\eta} = 0, \quad f = f_0 \\ \eta = \infty : \quad \frac{df}{d\eta} = 1 \end{aligned} \right\} \quad (2)$$

In this problem,  $\eta$  is a dimensionless space co-ordinate with value zero at the phase boundary,  $f$  is a dimensionless stream function,  $f_0$  has a specified value representing the mass flux through the phase boundary, while  $\beta$  is a quantity representative of the velocity-gradient in the main stream outside the boundary layer.

The quantities  $f_0$  and  $\beta$  are to be regarded as constants for a given solution; thus we are concerned with obtaining a two-parameter family of solutions. Both positive and negative real values of  $\beta$  and positive and negative, real and imaginary, values of  $f_0$  are of practical interest.

It has also been shown in Paper 1 that the most relevant properties of a particular solution include the values of the quantities on the left-hand sides of the following definitions:

$$f_0'' \equiv \left( \frac{d^2 f}{d\eta^2} \right)_{\eta=0} \quad (3)$$

$$\frac{\delta_2^2}{\nu} \frac{du_G}{dx} \equiv \beta \left[ \int_0^\infty \frac{df}{d\eta} \left( 1 - \frac{df}{d\eta} \right) d\eta \right]^2 \quad (4)$$

$$F_2 \equiv \frac{u_G}{\nu} \frac{d\delta_2^2}{dx} \equiv 2 \left( \frac{1}{\beta} - 1 \right) \frac{\delta_2^2}{\nu} \frac{du_G}{dx} \quad (5)$$

$$H_{12} \equiv \delta_1/\delta_2 \equiv \frac{\int_0^\infty (1 - df/d\eta)d\eta}{\int_0^\infty (df/d\eta)(1 - df/d\eta)d\eta} \quad (6)$$

$$H_{24} \equiv \delta_2/\delta_4 \equiv f_0'' \left\{ \int_0^\infty (df/d\eta)(1 - df/d\eta)d\eta \right\} \quad (7)$$

$$\frac{v_S \delta_2}{\nu} = -f_0 \left\{ \int_0^\infty (df/d\eta)(1 - df/d\eta)d\eta \right\}. \quad (8)$$

The right-hand sides of these definitions indicate plainly how the properties in question are to be computed once the solution of the equation is available in the form of the relation between  $f$  and  $\eta$ , for given  $f_0$  and  $\beta$ .

We shall be concerned, in the present paper, to provide graphs and tables of the functions appearing on the left of equations (3) to (8), either with  $f_0$  and  $\beta$  as arguments, or with alternative pairs.

### 1.3. Outline of present paper

The most important of the graphs and tables just mentioned appear in Section 3 (Tables 7 and 8, Figs. 4 and 5); they represent the only

parts of the present paper which need be considered by anyone solely concerned with the practical use of the calculation method of Paper 1 of the series.

Section 2 presents a survey of all the exact solutions to equation (1) which the authors have been able to find in the literature; it is these solutions which are used as the basis for the graphs and tables of Section 3. The latter have been derived from the former by interpolation.

The authors have not themselves obtained any new solutions to equation (1); however, the interpolation procedures and their results are believed to be novel. They have eliminated the need for all but confirmatory solutions over a considerable proportion of the region of practical interest.

## 2. SURVEY OF EXISTING SOLUTIONS

### 2.1. Remarks on terminology and notation

The six quantities on the left of equations (3) to (8) are, together with  $f_0$  and  $\beta$ , the ones which we find most convenient in calculations of the velocity boundary layer; the solutions to equation (1) will therefore be presented in terms of these quantities. However, boundary-layer solutions are often presented in different terms, so that a glossary becomes necessary.

This will now be provided. In particular we

conventional boundary-layer parameters involving "length Reynolds number",  $u_G x/\nu$ , into the present terminology. It will be remembered that, in Paper 1, it was noted that there are certain objections to referring the solution to a particular distance  $x$ , especially when the solution is to be used in conjunction with the hypothesis that the local boundary layer has no "memory" of how it originated. The latter supposition is implicit in the method of Paper 1.

The starting point of the transformation formulae is the equation for the free-stream velocity distribution which is characteristic of "similar" boundary layers, namely:

$$\frac{du_G}{dx} = C u_G^n \quad (9)$$

This equation, and the relation between  $n$  and  $\beta$ , namely:

$$\beta \equiv 1/(1 - n/2) \quad (10)$$

are explained in Paper 1. They permit the deductions (for  $n \neq 1$ ):

$$x = u_G \int \left\{ \frac{du_G}{dx} \left( \frac{2}{\beta} - 1 \right) \right\} \quad (11)$$

$$\frac{xu_G}{\nu} = u_G^2 \int \left\{ \nu \frac{du_G}{dx} \left( \frac{2}{\beta} - 1 \right) \right\} \quad (12)$$

$$c_f \sqrt{\frac{xu_G}{\nu}} = \frac{2}{\sqrt{[(2/\beta) - 1]}} \int \sqrt{\left( \frac{\delta_4^2}{\nu} \frac{du_G}{dx} \right)} \quad (13)$$

$$= \frac{2H_{24}}{\sqrt{[(2/\beta) - 1]}} \int \sqrt{\left( \frac{\delta_2^2}{\nu} \frac{du_G}{dx} \right)} \quad (14)$$

$$\frac{x}{\delta} \int \sqrt{\frac{xu_G}{\nu}} = \frac{1}{\sqrt{[(2/\beta) - 1]}} \int \sqrt{\left( \frac{\delta^2}{\nu} \frac{du_G}{dx} \right)} \quad (15)$$

$$\frac{v_S x}{\nu} \int \sqrt{\frac{xu_G}{\nu}} = \frac{(v_S \delta_2/\nu)}{\sqrt{[(2/\beta) - 1]}} \int \sqrt{\left( \frac{\delta_2^2}{\nu} \frac{du_G}{dx} \right)} \quad (16)$$

$$m = Eu = 1/(2/\beta - 1). \quad (17)$$

In this list the symbols on the left represent those conventionally used; those on the right represent the groupings which we have found convenient. Thus:

$x$  = distance from leading edge of a surface along which the main-stream velocity  $u_G$  varies in accordance with:

$Eu$  = Euler number, the exponent in equation (18), sometimes denoted by the symbol  $m$ .

$c_f$  = drag coefficient  $\equiv \tau_S g_0 / (\frac{1}{2} \rho u_G^2)$ .

where:

$\tau_S$  = local shear stress at wall (phase boundary),

$g_0$  = constant in Newton's Second Law of Motion,

$\rho$  = fluid density,

$u_G$  = local main-stream velocity,

$\delta$  = any boundary layer thickness, i.e. either displacement thickness  $\delta_1$ , momentum thickness,  $\delta_2$ , or shear thickness  $\delta_4$ .

Some of the above formulae become indeterminate when  $\beta = 0$ ; for  $du_G/dx$  is also zero for this case. They can therefore conveniently be

modified by substituting for  $du_G/dx$  from equation (5).

The formulae presented in this section have been used to translate published solutions of equation (1) into the terms of the present series of papers. They can of course also be used in the reverse direction.

In some cases, authors have not provided sufficient information in their publications for the desired quantities to be calculable from these formulae alone. In these cases we have, where possible, gone direct to the published relations between  $df/d\eta$  and  $\eta$ , evaluated the relevant quadratures, and obtained the desired quantities via equations (3) to (8).

## 2.2. Tabulation of solutions to equation (1)

The authors have searched the English and

German literatures for solutions to equation (1) with its appropriate boundary conditions. Only exact solutions have been considered. The relevant results are contained in the following tables. It will be noted that the important quantity  $(\delta_2^2/\nu)(du_G/dx)$  has not been tabulated throughout. This has been done to save space. This quantity can, however, easily be deduced from the tabulated values of  $F$  and  $\beta$  via equation (5). Where this is not possible because both  $\beta$  and  $F$  are zero, as in one part of Table 3,  $(\delta_2^2/\nu)(du_G/dx)$  has been tabulated in place of  $F$ . Solutions giving negative values of  $f_0''$  have been omitted as being without practical interest.

Table 1.  $f_0 = 0$ , various  $\beta$

This table, based on the work of Falkner [2, 3], with a few contributions from Mangler

Table 1. Boundary-layer parameters for:  $f_0 = 0$ , various  $\beta$

$\beta$	$f_0''$	$F_2$	$H_{12}$	$H_{24}$	$\frac{v_S \delta_2}{\nu}$	References
-4.0	$2.277\sqrt{-1}$	-0.4225	2.018	0.468	0.0	Mangler [4]
-1.0	$1.718\sqrt{-1}$	-1.540	1.752	0.674	0.0	ditto
-0.1988	0.0	0.821	4.030	0.0	0.0	Falkner [2, 3]
-0.19	0.0860	0.792	3.480	0.0496	0.0	ditto
-0.18	0.1285	0.760	3.297	0.0729	0.0	ditto
-0.16	0.1905	0.708	3.091	0.1052	0.0	ditto
-0.15	0.2161	0.681	3.020	0.1176	0.0	ditto
-0.14	0.2395	0.661	2.963	0.1290	0.0	ditto
-0.10	0.3191	0.583	2.800	0.1645	0.0	ditto
*-0.05	0.4008	0.508	2.672	0.1968	0.0	ditto
0.0	0.4696	0.441	2.591	0.2205	0.0	ditto
0.1	0.5870	0.342	2.481	0.2557	0.0	ditto
0.2	0.6869	0.266	2.412	0.2802	0.0	ditto
0.3	0.7748	0.208	2.361	0.2989	0.0	ditto
0.4	0.8542	0.1614	2.325	0.3132	0.0	ditto
0.5	0.9277	0.1226	2.297	0.3249	0.0	ditto
0.6	0.9960	0.0903	2.275	0.3344	0.0	ditto
0.8	1.1200	0.0389	2.241	0.3492	0.0	ditto
1.0	1.2326	0.0	2.217	0.3603	0.0	ditto
1.2	1.336	-0.0305	2.198	0.3690	0.0	ditto
1.4	1.431	-0.0550	2.184	0.3752	0.0	ditto
1.6	1.521	-0.0751	2.173	0.3807	0.0	ditto
1.8	1.606	-0.0921	2.163	0.3853	0.0	ditto
2.0	1.687	-0.1065	2.155	0.3893	0.0	ditto
2.2	1.764	-0.1188	2.149	0.3925	0.0	ditto
2.4	1.837	-0.1294	2.144	0.3949	0.0	ditto
$\infty$	1.1547	-0.2830	2.069	0.4344	0.0	Holstein [5]

\* The figures for this value of  $\beta$  appear to contain a small error but attempts to trace it were not successful.

[4] and Holstein [5], refers to boundary layers with zero mass transfer ( $f_0 = 0$ ). Some of the results overlap those of Hartree [6]. Since they are more extensive than Hartree's, and are quoted to a higher accuracy, Falkner's results have been preferred.

The solutions of Mangler involve imaginary values of the variables  $f$  and  $\eta$ . They were the only solutions of this class which could be found. Note that although  $f_0''$  is imaginary for these solutions,  $F_2$ ,  $H_{12}$ , and  $H_{24}$  are not.

Table 2.  $\beta = 0$ , various  $f_0$

This table is based on the work of Emmons

and Leigh [7]. It refers to boundary layers on bodies with finite mass transfer rate from the surface to the fluid ( $f_0 < 0$ ) or from the fluid to the surface ( $f_0 > 0$ ), with no gradient of main-stream velocity ( $du_G/dx = 0$ ). Additional values for larger  $f_0$  can be obtained from Table 4 below.

Table 3. Various  $\beta$  and  $f_0$

This table contains data abstracted from a variety of sources, and of varying accuracy. The data of Mangler [8] appear, on plotting, to be of lower accuracy than the others, but they are included because solutions for negative  $\beta$

Table 2. Boundary-layer parameters for:  $\beta = 0$ , various  $f_0$

$f_0$	$f_0''$	$F_2$	$H_{12}$	$H_{24}$	$\frac{v_S \delta_2}{v}$	References
-0.8757	0.0	1.5338	15.575	0.0	0.7669	Emmons and Leigh [7]
-0.8485	0.00475	1.4561	6.507	0.0040	0.7240	ditto
-0.7778	0.0244	1.2872	4.762	0.0196	0.6240	ditto
-0.7071	0.0502	1.1470	4.100	0.0380	0.5355	ditto
-0.6364	0.0805	1.0278	3.709	0.0577	0.4562	ditto
-0.5657	0.1143	0.9290	3.442	0.0777	0.3868	ditto
-0.4950	0.1512	0.8352	3.244	3.0977	0.3199	ditto
-0.4243	0.1907	0.7564	3.091	0.1173	0.2609	ditto
-0.3536	0.2326	0.6874	2.967	0.1364	0.2073	ditto
-0.2828	0.2766	0.6258	2.866	0.1547	0.1582	ditto
-0.2121	0.3225	0.5716	2.780	0.1724	0.1134	ditto
-0.1414	0.3700	0.5230	2.709	0.1892	0.0723	ditto
-0.0707	0.4191	0.4798	2.646	0.2053	0.0346	ditto
0.0	0.4696	0.4410	2.591	0.2205	0.0	ditto
0.0707	0.5214	0.4062	2.543	0.2350	-0.0319	ditto
0.1414	0.5743	0.3748	2.501	0.2486	-0.0612	ditto
0.2121	0.6284	0.3466	2.463	0.2616	-0.0883	ditto
0.2828	0.6834	0.3210	2.431	0.2738	-0.1133	ditto
0.3536	0.7394	0.2978	2.399	0.2853	-0.1364	ditto
0.4243	0.7962	0.2766	2.373	0.2961	-0.1578	ditto
0.4950	0.8538	0.2574	2.349	0.3063	-0.1776	ditto
0.5657	0.9121	0.2400	2.325	0.3160	-0.1960	ditto
0.6364	0.9711	0.2240	2.305	0.3250	-0.2130	ditto
0.7071	1.0308	0.2096	2.287	0.3337	-0.2289	ditto
0.7778	1.0910	0.1962	2.270	0.3417	-0.2436	ditto
0.8485	1.1518	0.1838	2.254	0.3493	-0.2574	ditto
0.9192	1.2131	0.1726	2.239	0.3565	-0.2702	ditto
0.9899	1.2748	0.1660	2.226	0.3632	-0.2820	ditto
1.0607	1.3370	0.1526	2.214	0.3694	-0.2931	ditto
1.4142	1.6538	0.1150	2.164	0.3963	-0.3388	ditto
1.7678	1.9782	0.0886	2.129	0.4162	-0.3719	ditto
2.1213	2.3083	0.0700	2.104	0.4317	-0.3967	ditto
2.8284	2.9803	0.0462	2.070	0.4527	-0.4296	ditto
3.5355	3.6627	0.0324	2.051	0.4659	-0.4497	ditto
4.2426	4.3516	0.0278	2.037	0.4743	-0.4624	ditto
7.0711	7.1397	0.0094	2.012	0.4898	-0.4851	ditto

are scarce. The physical significance of the various values of  $\beta$  is discussed below (Section 3.3).

Table 4. Asymptotic solutions

Pretsch [14] and Watson [15] have published solutions which are valid for values of  $f_0$  which are either very large positively or very

small negatively. The data in Table 4 are based on their work. Since the solutions are only asymptotically correct, the data for moderate values of  $f_0$  must be regarded as approximate.

Tables 5 and 6. Incomplete solutions

Some solutions are available for which the

Table 3. Boundary-layer parameters for: various  $\beta$  and  $f_0$

$\beta$	$f_0$	$f_0''$	$F_2$	$H_{12}$	$H_{24}$	$\frac{v_s \delta_2}{\nu}$	References
-0.25	0.193	0.176	0.644	3.135	0.0903	-0.0990	Mangler [8]
-0.25	0.305	0.344	0.592	2.679	0.1675	-0.1485	ditto
-0.25	1.231	1.285	0.200	2.236	0.3624	-0.3471	ditto
-0.10	-0.180	0.170	0.781	3.120	0.1013	0.1073	ditto
-0.10	-0.135	0.220	0.735	2.855	0.1272	0.0780	ditto
-0.10	0.289	0.565	0.4026	2.544	0.2418	-0.1237	ditto
-0.10	0.595	0.830	0.2772	2.380	0.2946	-0.2112	ditto
-0.10	1.022	1.200	0.1628	2.445	0.3259	-0.2776	ditto
-0.08725	-0.3461	0.0	0.9520	4.468	0.0	0.2291	Brown and Donoughe [9]
-0.0145	-0.7046	0.0	1.238	5.770	0.0	0.5505	ditto
0.0952	-0.7246	0.1956	0.7955	3.055	0.1290	0.4804	ditto
0.2	-1.0896	0.2028	0.8244	3.004	0.1456	0.7821	Schaefer [10]
0.2	-0.6993	0.3208	0.5448	2.743	0.1872	0.4080	ditto
0.2	-0.3461	0.4833	0.3761	2.550	0.2343	0.1678	ditto
0.2	0.3731	0.9432	0.1884	2.306	0.3237	-0.1281	ditto
0.2	1.2543	1.6463	0.0924	2.163	0.3954	-0.3012	ditto
0.2	2.6087	2.8620	0.0394	2.079	0.4484	-0.4087	ditto
0.2	4.7806	4.9364	0.0152	2.031	0.4791	-0.4639	ditto
0.2509	-0.7583	0.3565	0.4788	2.672	0.2031	0.4320	Brown and Donoughe [9]
0.6667	-1.7321	0.3747	0.2601	2.561	0.2340	1.0815	Eckert, Donoughe, Moore [11]
0.6667	-0.8660	0.6172	0.1371	2.406	0.2799	0.3927	Donoughe, Livingood [12]
0.6667	-0.4330	0.8053	0.0988	2.327	0.3099	0.1666	ditto
1.0	-4.3346	0.2300	0.9912	2.585	0.2290	4.3155	Schlichting, Bussmann [13]
1.0	-3.1905	0.3106	0.5949	2.539	0.2396	2.4608	ditto
1.0	-3.0	0.3294	0.5413	2.526	0.2424	2.2071	Eckert, Donoughe, Moore [11]
1.0	-2.0	0.4758	0.3104	2.444	0.2651	1.1142	ditto
1.0	-1.198	0.6864	0.1877	2.350	0.2973	0.5190	Schlichting, Bussmann [13]
1.0	-1.0	0.7565	0.1647	2.329	0.3070	0.4058	Donoughe, Livingood [12]
1.0	-0.5	0.9692	0.1185	2.267	0.3337	0.1722	ditto
1.0	-0.1107	1.171	0.0920	2.230	0.3552	0.0336	Schlichting, Bussmann [13]
1.0	0.5	1.5418	0.0625	2.217	0.3853	-0.1248	ditto
1.0	1.095	1.9550	0.0436	2.126	0.4082	-0.2286	ditto
1.0	1.9265	2.6080	0.0279	2.088	0.4353	-0.3215	ditto
1.0	2.664	3.2400	0.0195	2.077	0.4523	-0.3719	ditto
$\infty$	$-10.0\sqrt{\beta}$	$0.1000\sqrt{\beta}$	-11.394	2.252	0.3106	31.06	Holstein [5]
$\infty$	$-4.0\sqrt{\beta}$	$0.2482\sqrt{\beta}$	-3.4848	2.218	0.3276	5.280	ditto
$\infty$	$-2.0\sqrt{\beta}$	$0.4638\sqrt{\beta}$	-1.2136	2.163	0.3613	1.558	ditto
$\infty$	$2.0\sqrt{\beta}$	$2.5644\sqrt{\beta}$	-0.0698	2.023	0.4788	-0.3734	ditto
$\infty$	$4.0\sqrt{\beta}$	$4.3408\sqrt{\beta}$	-0.0256	2.013	0.4909	-0.4524	ditto
* $\infty$	$10.0\sqrt{\beta}$	$10.1474\sqrt{\beta}$	0.0048	2.022	0.4950	-0.4878	ditto

\* The figures for this value of  $\beta$  appear to contain a small error but attempts to trace it were not successful.

Table 4. Boundary-layer parameters obtained from formulae which are asymptotically correct for large values of  $|f_0|$ : various  $\beta$  and  $f_0$

$f_0$	$\beta$	$f_0''$	$F_2$	$H_{12}$	$H_{24}$	$\frac{v_s \delta_2}{\nu}$	References
$-\infty$	-2.0	0.0	$-\infty$	2.065	0.3844	$\infty$	Pretsch [14]
$-\infty$	-1.0	0.0	$-\infty$	1.752	0.5708		ditto
$-\infty$	0.0	0.0		$\infty$	0.0	$\infty$	ditto
$-\infty$	0.1			4.85	0.632		ditto
$-\infty$	0.125			4.47	0.0743		ditto
$-\infty$	0.1667			4.13	0.0888		ditto
$-\infty$	0.20			3.82	0.1018		ditto
$-\infty$	0.25			3.571	0.1167		ditto
$-\infty$	0.333			3.30	0.1370		ditto
$-\infty$	0.5			3.0	0.1667		ditto
$-\infty$	1.0			2.66	0.2146		ditto
$-\infty$	1.5			2.536	0.2378		ditto
$-\infty$	2.0			2.475	0.2512		ditto
$-\infty$	$\infty$			2.29	0.3165		ditto
2.5	-1.5	1.5879	0.3016	2.18	0.39	-0.614	Watson [15]
2.5	-1.25	1.8459	0.2242	2.147	0.412	-0.558	ditto
2.5	-1.0	2.0617	0.1701	2.125	0.4252	-0.5156	ditto
2.5	-0.75	2.2448	0.1290	2.113	0.431	-0.480	ditto
2.5	-0.5	2.3889	0.0972	2.11	0.43	-0.450	ditto
2.5	-0.25	2.5610	0.0672	2.12	0.42	-0.410	ditto
2.5	0.0			2.13			ditto
5.0	-4.0			2.023			ditto
5.0	-3.0	4.0164	0.0595	2.026	0.49	-0.61	ditto
5.0	-2.0	4.4505	0.0358	2.027	0.486	-0.546	ditto
5.0	-1.5	4.6291	0.0274	2.0273	0.4843	-0.5231	ditto
5.0	-1.25	4.7144	0.0237	2.0275	0.4836	-0.5129	ditto
5.0	-1.0	4.7954	0.0203	2.0276	0.4829	-0.5035	ditto
5.0	-0.75	4.8747	0.01713	2.0278	0.4823	-0.4947	ditto
5.0	-0.5	4.9496	0.01420	2.0281	0.4815	-0.4864	ditto
5.0	-0.25	5.0209	0.01147	2.0285	0.481	-0.479	ditto
5.0	0.0	5.0955	0.00887	2.0289	0.480	-0.471	ditto
5.0	0.25	5.1616	0.00646	2.0294	0.479	-0.464	ditto
5.0	0.5	5.2298	0.00418	2.030	0.478	-0.457	ditto
5.0	0.75	5.3000	0.002025	2.031	0.477	-0.450	ditto
5.0	1.0	5.3612	0.0	2.032	0.475	-0.443	ditto
5.0	1.25	5.3409	-0.001936	2.034	0.47	-0.44	ditto
5.0	1.50	5.4651	-0.003698	2.035	0.47	-0.43	ditto
5.0	2.0	5.6098	-0.006724	2.04	0.46	-0.41	ditto
10.0	-6.0	9.0485	0.04343	1.999	0.504	-0.557	ditto
10.0	-4.0	9.4152	0.02828	2.0023	0.5007	-0.5318	ditto
10.0	-3.0	9.5832	0.02168	2.00392	0.4989	-0.5206	ditto
10.0	-2.0	9.7443	0.01563	2.00538	0.49729	-0.51034	ditto
10.0	-1.5	9.8226	0.01278	2.00606	0.49653	-0.50550	ditto
10.0	-1.25	9.8613	0.01139	2.00640	0.49617	-0.50315	ditto
10.0	-1.0	9.8996	0.01003	2.00672	0.49581	-0.50084	ditto
10.0	-0.75	9.9374	0.008700	2.00704	0.49546	-0.49858	ditto
10.0	-0.5	9.9750	0.007391	2.00736	0.49511	-0.49635	ditto
10.0	-0.25	10.0123	0.006105	2.00767	0.49478	-0.49417	ditto
10.0	0.0	10.0492	0.004842	2.00797	0.49444	-0.49202	ditto
10.0	0.25	10.0857	0.003600	2.00827	0.49411	-0.48991	ditto
10.0	0.50	10.1230	0.002379	2.00856	0.4938	-0.4878	ditto
10.0	0.75	10.1585	0.001180	2.00886	0.4935	-0.4858	ditto

Table 4—continued

$f_0$	$\beta$	$f''_0$	$F_2$	$H_{12}$	$H_{24}$	$\frac{v_s \delta_2}{v}$	References
10.0	1.0	10.1943	0.0	2.0091	0.4932	-0.4838	Watson [15]
10.0	1.25	10.2304	-0.001161	2.0094	0.4929	-0.4818	ditto
10.0	1.5	10.2646	-0.002303	2.0097	0.4926	-0.4799	ditto
10.0	2.0	10.3361	-0.004532	2.0102	0.492	-0.476	ditto
20.0	-18.0	18.5375	0.028424	1.99350	0.507	-0.547	ditto
20.0	-10.0	19.2352	0.015044	1.99775	0.503	-0.523	ditto
20.0	-6.0	19.5646	0.009183	1.99959	0.50108	-0.51223	ditto
20.0	-4.0	19.7209	0.006433	2.00045	0.50020	-0.50728	ditto
20.0	-3.0	19.7980	0.005098	2.00087	0.49978	-0.50488	ditto
20.0	-2.0	19.8742	0.003788	2.00127	0.49936	-0.50252	ditto
20.0	-1.5	19.9122	0.003142	2.00147	0.49916	-0.50136	ditto
20.0	-1.25	19.9309	0.002821	2.00157	0.49905	-0.50078	ditto
20.0	-1.0	19.9500	0.002502	2.00167	0.49896	-0.50021	ditto
20.0	-0.75	19.9688	0.002184	2.00177	0.49886	-0.49964	ditto
20.0	-0.50	19.9876	0.001868	2.00187	0.49876	-0.49907	ditto
20.0	-0.25	20.0060	0.001550	2.00196	0.49820	-0.49805	ditto
20.0	0.0	20.0249	0.001240	2.00206	0.49856	-0.49794	ditto
20.0	0.25	20.0434	0.000928	2.00216	0.49846	-0.49738	ditto
20.0	0.75	20.0806	0.000308	2.00235	0.49827	-0.49627	ditto
20.0	1.0	20.0993	0.0	2.00244	0.49817	-0.49571	ditto
20.0	1.25	20.1175	-0.000306	2.00253	0.49807	-0.49516	ditto
20.0	1.5	20.1359	-0.000612	2.00263	0.49797	-0.49461	ditto
20.0	2.0	20.1726	-0.001218	2.00281	0.49779	-0.49353	ditto
$\infty$	all	$\infty$		2.00	0.500		Pretsch [14]

Table 5. Values of  $f''_0$  for various  $\beta$  and  $f_0$  (Bain [16])

$f_0 \backslash \beta$	0.0	0.25	0.5	0.75	1.0	1.5	2.0
3.0	3.145	3.248	3.346	3.438	3.527	3.692	3.846
2.5	2.667	2.783	2.892	2.995	3.091	3.270	3.435
2.0	2.194	2.329	2.451	2.564	2.670	2.864	3.040
1.5	1.732	1.888	2.026	2.152	2.268	2.477	2.663
1.0	1.284	1.467	1.624	1.763	1.889	2.113	2.310
0.5	0.8579	1.077	1.254	1.406	1.542	1.778	1.983
0.0	0.4697	0.7319	0.9277	1.090	1.233	1.477	1.687
-0.5	0.1485				0.9692		
-1.0					0.7565		
-1.5					0.5943		
-2.0					0.4758		
-2.5					0.3909		
-3.0					0.3295		
-3.5					0.2839		
-4.0					0.2490		
-4.5					0.2217		
-5.0					0.1997		



Table 6. Pairs of values of  $f_0$  and  $\beta$  giving  $f_0'' = 0$  (Watson [15])

$\beta$	-18.0	-10.0	-6.0	-4.0	-3.0	-2.0	-1.5	-1.25	-1.0	-0.1988	0.0
$f_0$	10.85	7.815	5.745	4.392	3.563	2.572	2.023	*1.767	1.414	0.0	-0.876

\* This figure appears to contain a small error but attempts to trace it were not successful.

quadratures appearing in equations (4) and (6) have not been evaluated, either because of the inaccessibility or the inadequate accuracy of the data. Tables 5 and 6 are based on these. They are included here because they deal with cases of particular interest: Table 5 covers a range of  $\beta$  and  $f_0$  values not considered by other authors; Table 6 provides solutions having zero values of  $f_0''$ . (Other complete solutions with  $f_0'' = 0$  can be found in Table 3).

2.3. Discussion of the currently available exact solutions

Figure 1 indicates, by means of lines drawn on a graph of  $\beta$  versus  $f_0$ , the range of conditions for which exact solutions giving non-negative  $f_0''$  are available. The full lines represent complete solutions (i.e. those including reference to  $\delta_2$ ); the broken lines represent incomplete solutions. Watson's asymptotic solutions have been marked

as full lines (the verticals for  $f_0 = 2.5, 5.0, 10.0, 20.0$ ), even though their accuracy is questionable at the lower values of  $f_0$ .

Two isolated points appear on the  $f_0 = 0$  line below the curve marked "separation",\* which is the locus of all solutions giving  $f_0'' = 0$ . Since we have already asserted that only solutions giving non-negative  $f_0''$  are recorded, the presence of these points may raise the question

of whether the "separation" locus doubles back on itself so as to place these points in the  $f_0'' > 0$  region.

The answer to the question appears to be "no". The solution to the resulting paradox is that the two points in question do not really belong on Fig. 1 at all but on a separate figure valid for

\* The line is so named because it is a fact of experience that a vanishing of the wall shear stress ( $f_0'' = 0$ ) is usually followed by the flow pattern known as "separation of the boundary layer from the wall".

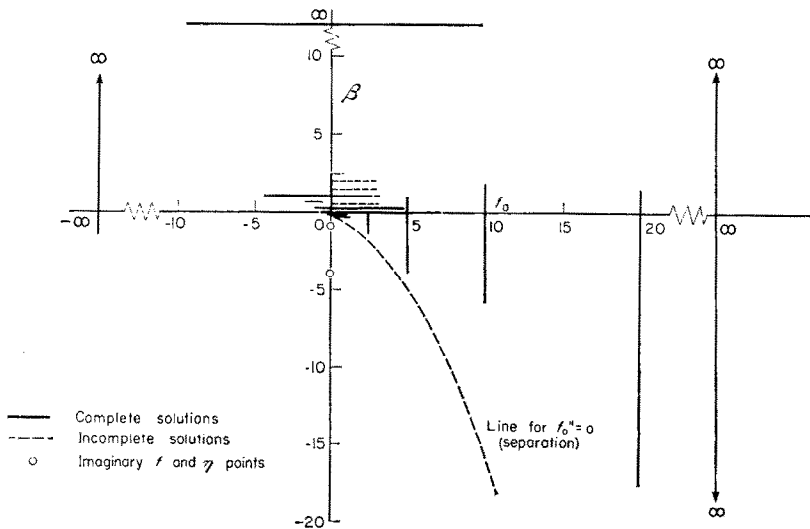


FIG. 1. Chart showing the availability of exact solutions of the velocity equation of the laminar boundary layer. Some of the available solutions in the neighbourhood of the origin have been omitted for greater clarity.





Table 8. Values of  $F_2$  and  $(\delta_2^2/\nu) du_G/dx$  derived from figure i.

$\frac{v_S \delta_2}{\nu}$ $\beta$	-0.49	-0.48	-0.47	-0.46	-0.45	-0.40	-0.35	-0.30	-0.25	-0.20	-0.15	-0.10	-0.05	0.0
-0.25	0.0101	0.0195	0.0292	0.0370	0.0493									
-0.20	-0.0010	-0.0020	-0.0029	-0.0037	-0.0049									
-0.15	-0.0008	-0.0015	-0.0022	-0.0030	-0.0038									
-0.10	-0.0006	-0.0010	-0.0016	-0.0022	-0.0027									
-0.05	-0.0003	-0.0007	-0.0010	-0.0014	-0.0017									
0.0	0.0060	0.0124	0.0186	0.0252	0.0320	0.0674	0.1062	0.1468	0.1904	0.2364	0.2840	0.3344	0.3870	0.4410
0.10	0.0050	0.0097	0.0148	0.0203	0.0256	0.0540	0.0844	0.1163	0.1496	0.1858	0.2236	0.2617	0.3015	0.3415
0.20	0.0003	0.0005	0.0008	0.0011	0.0014	0.0030	0.0047	0.0065	0.0083	0.0103	0.0124	0.0145	0.0167	0.0190
0.30	0.0000	0.0000	0.0000	0.0000	0.0000	0.0000	0.0000	0.0000	0.0000	0.0000	0.0000	0.0000	0.0000	0.0000
0.40	0.0007	0.0014	0.0019	0.0028	0.0036	0.0074	0.0114	0.0156	0.0201	0.0247	0.0294	0.0344	0.0394	0.0446
0.50	0.0008	0.0017	0.0025	0.0035	0.0044	0.0090	0.0139	0.0191	0.0244	0.0300	0.0356	0.0414	0.0475	0.0538
0.60	0.0010	0.0020	0.0029	0.0041	0.0052	0.0104	0.0161	0.0219	0.0281	0.0344	0.0407	0.0474	0.0542	0.0613
0.80	0.0011	0.0022	0.0033	0.0046	0.0057	0.0116	0.0179	0.0243	0.0312	0.0382	0.0451	0.0524	0.0599	0.0677
1.0	0.0006	0.0013	0.0019	0.0027	0.0033	0.0068	0.0104	0.0142	0.0181	0.0221	0.0261	0.0303	0.0346	0.0389
1.2	0.0013	0.0026	0.0039	0.0053	0.0067	0.0136	0.0208	0.0283	0.0362	0.0442	0.0522	0.0605	0.0691	0.0778
1.4	0.0014	0.0029	0.0045	0.0060	0.0075	0.0152	0.0231	0.0314	0.0399	0.0488	0.0578	0.0669	0.0761	0.0854
1.6	-0.0005	-0.0010	-0.0016	-0.0022	-0.0027	-0.0055	-0.0083	-0.0113	-0.0144	-0.0175	-0.0208	-0.0239	-0.0272	-0.0305
1.8	0.0016	0.0031	0.0047	0.0065	0.0081	0.0165	0.0250	0.0339	0.0431	0.0525	0.0623	0.0718	0.0817	0.0914
2.0	-0.0010	-0.0019	-0.0029	-0.0040	-0.0050	-0.0100	-0.0152	-0.0206	-0.0261	-0.0318	-0.0376	-0.0434	-0.0493	-0.0550
2.2	0.0017	0.0033	0.0050	0.0070	0.0087	0.0175	0.0265	0.0360	0.0457	0.0556	0.0658	0.0759	0.0862	0.0963
2.4	-0.0013	-0.0026	-0.0040	-0.0055	-0.0068	-0.0138	-0.0209	-0.0283	-0.0358	-0.0436	-0.0516	-0.0594	-0.0673	-0.0751
2.6	0.0017	0.0035	0.0053	0.0073	0.0091	0.0184	0.0278	0.0378	0.0478	0.0581	0.0688	0.0792	0.0898	0.1002
2.8	-0.0016	-0.0032	-0.0049	-0.0067	-0.0084	-0.0170	-0.0258	-0.0349	-0.0441	-0.0536	-0.0633	-0.0728	-0.0826	-0.0921
3.0	0.0018	0.0036	0.0055	0.0076	0.0095	0.0191	0.0290	0.0393	0.0496	0.0603	0.0712	0.0819	0.0929	0.1036
3.2	-0.0019	-0.0038	-0.0057	-0.0078	-0.0098	-0.0198	-0.0299	-0.0406	-0.0511	-0.0621	-0.0733	-0.0842	-0.0955	-0.1065
3.4	0.0019	0.0038	0.0057	0.0078	0.0098	0.0198	0.0299	0.0406	0.0511	0.0621	0.0733	0.0842	0.0955	0.1065
3.6	-0.0021	-0.0043	-0.0064	-0.0088	-0.0110	-0.0222	-0.0335	-0.0454	-0.0573	-0.0695	-0.0818	-0.0941	-0.1066	-0.1188
3.8	0.0019	0.0039	0.0059	0.0081	0.0101	0.0203	0.0307	0.0416	0.0525	0.0637	0.0750	0.0862	0.0977	0.1089
4.0	-0.0023	-0.0047	-0.0070	-0.0096	-0.0120	-0.0243	-0.0366	-0.0497	-0.0625	-0.0758	-0.0894	-0.1027	-0.1163	-0.1294
4.2	0.0020	0.0040	0.0060	0.0082	0.0103	0.0209	0.0314	0.0426	0.0536	0.0650	0.0766	0.0880	0.0997	0.1109
4.4	-0.0025	-0.0051	-0.0075	-0.0103	-0.0129	-0.0262	-0.0394	-0.0534	-0.0672	-0.0815	-0.0959	-0.1103	-0.1247	-0.1390
4.6	0.0020	0.0041	0.0061	0.0084	0.0105	0.0213	0.0320	0.0434	0.0546	0.0662	0.0779	0.0896	0.1013	0.1129
4.8	-0.0027	-0.0054	-0.0080	-0.0110	-0.0137	-0.0278	-0.0419	-0.0568	-0.0715	-0.0865	-0.1017	-0.1169	-0.1322	-0.1473
5.0	0.0021	0.0042	0.0062	0.0085	0.0107	0.0216	0.0326	0.0442	0.0556	0.0673	0.0791	0.0909	0.1028	0.1146
5.2	-0.0028	-0.0056	-0.0085	-0.0116	-0.0145	-0.0293	-0.0441	-0.0597	-0.0752	-0.0909	-0.1069	-0.1228	-0.1389	-0.1547
5.4	0.0021	0.0042	0.0064	0.0087	0.0109	0.0220	0.0331	0.0448	0.0564	0.0682	0.0802	0.0921	0.1042	0.1160
5.6	-0.0034	-0.0067	-0.0101	-0.0136	-0.0171	-0.0348	-0.0522	-0.0706	-0.0891	-0.1074	-0.1260	-0.1449	-0.1637	-0.1822
5.8	0.0023	0.0045	0.0067	0.0091	0.0114	0.0232	0.0348	0.0471	0.0594	0.0716	0.0840	0.0966	0.1091	0.1215
6.0	-0.0037	-0.0074	-0.0112	-0.0150	-0.0189	-0.0382	-0.0576	-0.0778	-0.0978	-0.1179	-0.1384	-0.1590	-0.1797	-0.2000
6.2	0.0023	0.0046	0.0070	0.0094	0.0118	0.0239	0.0360	0.0486	0.0611	0.0737	0.0865	0.0994	0.1123	0.1250
6.4	-0.0040	-0.0078	-0.0119	-0.0160	-0.0200	-0.0408	-0.0613	-0.0827	-0.1040	-0.1253	-0.1470	-0.1690	-0.1908	-0.2125
6.6	0.0024	0.0047	0.0071	0.0096	0.0120	0.0245	0.0368	0.0496	0.0624	0.0752	0.0882	0.1014	0.1145	0.1275
6.8	-0.0041	-0.0082	-0.0125	-0.0167	-0.0209	-0.0425	-0.0641	-0.0864	-0.1085	-0.1308	-0.1534	-0.1764	-0.1990	-0.2217
7.0	0.0024	0.0048	0.0073	0.0098	0.0122	0.0248	0.0374	0.0504	0.0633	0.0763	0.0895	0.1029	0.1161	0.1293
7.2	-0.0042	-0.0084	-0.0129	-0.0173	-0.0216	-0.0440	-0.0662	-0.0893	-0.1120	-0.1351	-0.1584	-0.1820	-0.2054	-0.2287
7.4	0.0024	0.0048	0.0074	0.0099	0.0124	0.0251	0.0378	0.0510	0.0640	0.0772	0.0905	0.1040	0.1174	0.1307
7.6	-0.0043	-0.0087	-0.0132	-0.0177	-0.0222	-0.0450	-0.0679	-0.0916	-0.1148	-0.1384	-0.1621	-0.1863	-0.2105	-0.2343
7.8	0.0024	0.0049	0.0074	0.0100	0.0125	0.0253	0.0382	0.0515	0.0646	0.0779	0.0912	0.1048	0.1184	0.1318
8.0	-0.0045	-0.0088	-0.0135	-0.0181	-0.0226	-0.0459	-0.0693	-0.0932	-0.1172	-0.1412	-0.1654	-0.1901	-0.2146	-0.2389
8.2	0.0025	0.0049	0.0075	0.0100	0.0126	0.0255	0.0385	0.0518	0.0651	0.0784	0.0919	0.1056	0.1192	0.1327
8.4	-0.0049	-0.0097	-0.0147	-0.0197	-0.0247	-0.0501	-0.0758	-0.1016	-0.1279	-0.1539	-0.1801	-0.2069	-0.2337	-0.2603
8.6	0.0026	0.0051	0.0077	0.0104	0.0130	0.0264	0.0399	0.0535	0.0673	0.0810	0.0948	0.1089	0.1230	0.1370
∞	-0.0053	-0.0106	-0.0160	-0.0215	-0.0269	-0.0546	-0.0826	-0.1108	-0.1390	-0.1674	-0.1958	-0.2248	-0.2538	-0.2830
	0.0027	0.0053	0.0080	0.0107	0.0135	0.0273	0.0413	0.0554	0.0695	0.0837	0.0979	0.1124	0.1269	0.1415

Table 7. [N.B. of each pair, the top figure is  $F_2$ , the bottom  $(\delta_2^2/\nu) du_G/dx$ ]

0.1	0.2	0.3	0.4	0.5	0.6	0.7	0.8	0.9	1.0	1.5	2.0	2.5	3.0	$\frac{v_G \delta_2}{\nu}$ $\beta$
														-0.25
														-0.20
														-0.15
														-0.10
														-0.05
0.5550	0.6780	0.8090	0.9480	1.0936	1.2490	1.4160	1.6000	1.8000	2.0000	3.0000	4.0000	5.0000	6.0000	0.0
0.0	0.0	0.0	0.0	0.0	0.0	0.0	0.0	0.0	0.0	0.0	0.0	0.0	0.0	0.10
0.4247	0.5141	0.6060	0.7028	0.8038	0.9079	1.0123	0.9079	1.0123	0.9079	1.3800	1.7700	2.1560	2.5520	0.20
0.0236	0.0286	0.0337	0.0390	0.0447	0.0504	0.0562	0.6122	0.6864	0.7618	0.8382	0.9142	0.9911	1.0680	0.30
0.3304	0.3978	0.4672	0.5390	0.6122	0.6864	0.7618	0.8382	0.9142	0.9911	1.0680	1.1450	1.2220	1.3000	0.40
0.0413	0.0497	0.0584	0.0674	0.0765	0.0858	0.0952	0.1048	0.1143	0.1239	0.1725	0.2213	0.2695	0.3190	0.50
0.2571	0.3081	0.3611	0.4145	0.4689	0.5243	0.5808	0.6374	0.6944	0.7512	1.0380	1.3270	1.6210	1.9150	0.60
0.0551	0.0660	0.0774	0.0888	0.1005	0.1124	0.1245	0.1366	0.1488	0.1610	0.2225	0.2844	0.3474	0.4103	0.70
0.1990	0.2379	0.2771	0.3177	0.3584	0.4004	0.4424	0.4850	0.5282	0.5710	0.7851	1.0040	1.2220	1.4420	0.80
0.0663	0.0793	0.0924	0.1059	0.1195	0.1335	0.1475	0.1617	0.1761	0.1903	0.2617	0.3347	0.4075	0.4808	0.90
0.1511	0.1801	0.2096	0.2397	0.2700	0.3010	0.3326	0.3645	0.3965	0.4283	0.5871	0.7495	0.9132	1.0760	1.0
0.0756	0.0900	0.1048	0.1199	0.1350	0.1505	0.1663	0.1822	0.1982	0.2141	0.2938	0.3747	0.4566	0.5380	1.1
0.1110	0.1321	0.1535	0.1754	0.1973	0.2196	0.2425	0.2655	0.2887	0.3118	0.4271	0.5445	0.6627	0.7802	1.2
0.0832	0.0991	0.1152	0.1315	0.1480	0.1647	0.1819	0.1992	0.2165	0.2338	0.3203	0.4084	0.4970	0.5852	1.3
0.0477	0.0566	0.0657	0.0749	0.0843	0.0936	0.1031	0.1128	0.1224	0.1321	0.1807	0.2299	0.2792	0.3285	1.4
0.0954	0.1133	0.1314	0.1498	0.1685	0.1871	0.2063	0.2256	0.2447	0.2643	0.3614	0.4598	0.5584	0.6570	1.5
0.0	0.0	0.0	0.0	0.0	0.0	0.0	0.0	0.0	0.0	0.0	0.0	0.0	0.0	1.6
0.1045	0.1239	0.1435	0.1634	0.1838	0.2041	0.2247	0.2451	0.2657	0.2867	0.3919	0.4975	0.6032	0.7093	1.7
-0.0372	-0.0441	-0.0510	-0.0580	-0.0652	-0.0724	-0.0796	-0.0868	-0.0939	-0.1013	-0.1382	-0.1754	-0.2126	-0.2496	1.8
0.1117	0.1322	0.1529	0.1741	0.1957	0.2171	0.2389	0.2603	0.2818	0.3040	0.4147	0.5262	0.6378	0.7489	1.9
-0.0671	-0.0793	-0.0918	-0.1044	-0.1173	-0.1300	-0.1429	-0.1556	-0.1685	-0.1815	-0.2474	-0.3137	-0.3797	-0.4458	2.0
0.1174	0.1388	0.1606	0.1827	0.2052	0.2274	0.2501	0.2723	0.2948	0.3177	0.4329	0.5490	0.6645	0.7802	2.1
-0.0915	-0.1083	-0.1251	-0.1423	-0.1596	-0.1768	-0.1945	-0.2116	-0.2289	-0.2467	-0.3357	-0.4256	-0.5150	-0.6041	2.2
0.1220	0.1444	0.1668	0.1897	0.2128	0.2358	0.2593	0.2821	0.3052	0.3289	0.4476	0.5675	0.6867	0.8055	2.3
-0.1120	-0.1324	-0.1529	-0.1738	-0.1948	-0.2157	-0.2371	-0.2581	-0.2789	-0.3005	-0.4087	-0.5179	-0.6263	-0.7342	2.4
0.1322	0.1562	0.1799	0.2045	0.2291	0.2535	0.2784	0.3028	0.3273	0.3525	0.4786	0.6059	0.7323	0.8580	2.5
-0.1572	-0.1857	-0.2137	-0.2428	-0.2721	-0.3009	-0.3305	-0.3594	-0.3884	-0.4180	-0.5673	-0.7180	-0.8674	-1.0163	2.6
0.1347	0.1592	0.1831	0.2081	0.2332	0.2579	0.2833	0.3080	0.3329	0.3583	0.4863	0.6154	0.7435	0.8711	2.7
-0.1684	-0.1990	-0.2289	-0.2600	-0.2912	-0.3220	-0.3535	-0.3845	-0.4154	-0.4470	-0.6064	-0.7671	-0.9265	-1.0859	2.8
0.1369	0.1617	0.1859	0.2112	0.2366	0.2616	0.2872	0.3124	0.3375	0.3631	0.4927	0.6233	0.7528	0.8822	2.9
-0.1785	-0.2109	-0.2433	-0.2753	-0.3083	-0.3409	-0.3741	-0.4067	-0.4393	-0.4727	-0.6410	-0.8105	-0.9787	-1.1470	3.0
0.1389	0.1640	0.1885	0.2141	0.2398	0.2651	0.2910	0.3163	0.3417	0.3676	0.4986	0.6304	0.7612	0.8921	3.1
-0.1875	-0.2214	-0.2543	-0.2887	-0.3234	-0.3575	-0.3922	-0.4265	-0.4606	-0.4956	-0.6717	-0.8489	-1.0248	-1.2012	3.2
0.1406	0.1661	0.1908	0.2165	0.2425	0.2681	0.2942	0.3198	0.3454	0.3717	0.5038	0.6367	0.7686	0.9009	3.3
-0.2208	-0.2600	-0.2988	-0.3387	-0.3789	-0.4187	-0.4591	-0.4989	-0.5388	-0.5793	-0.7839	-0.9897	-1.1940	-1.3988	3.4
0.1470	0.1733	0.1992	0.2258	0.2526	0.2791	0.3061	0.3326	0.3592	0.3862	0.5226	0.6598	0.7960	0.9325	3.5
-0.2418	-0.2849	-0.3274	-0.3708	-0.4146	-0.4579	-0.5020	-0.5455	-0.5888	-0.6328	-0.8554	-1.0790	-1.3014	-1.5240	3.6
0.1511	0.1781	0.2046	0.2317	0.2591	0.2862	0.3137	0.3409	0.3680	0.3955	0.5346	0.6744	0.8134	0.9525	3.7
-0.2367	-0.3022	-0.3474	-0.3932	-0.4394	-0.4853	-0.5316	-0.5777	-0.6237	-0.6700	-0.9051	-1.1407	-1.3753	-1.6109	3.8
0.1540	0.1813	0.2084	0.2359	0.2636	0.2912	0.3189	0.3466	0.3742	0.4020	0.5430	0.6844	0.8252	0.9665	3.9
-0.2679	-0.3149	-0.3621	-0.4098	-0.4577	-0.5054	-0.5534	-0.6012	-0.6493	-0.6974	-0.9408	-1.1860	-1.4299	-1.6746	4.0
0.1562	0.1837	0.2112	0.2390	0.2670	0.2948	0.3228	0.3507	0.3787	0.4068	0.5488	0.6918	0.8341	0.9768	4.1
-0.2765	-0.3250	-0.3736	-0.4226	-0.4719	-0.5210	-0.5705	-0.6196	-0.6688	-0.7185	-0.9689	-1.2207	-1.4714	-1.7234	4.2
0.1580	0.1857	0.2135	0.2415	0.2697	0.2977	0.3260	0.3540	0.3822	0.4106	0.5537	0.6975	0.8408	0.9848	4.3
-0.2831	-0.3330	-0.3824	-0.4327	-0.4831	-0.5333	-0.5836	-0.6341	-0.6845	-0.7350	-0.9903	-1.2477	-1.5043	-1.7617	4.4
0.1593	0.1873	0.2151	0.2434	0.2717	0.3000	0.3283	0.3567	0.3851	0.4134	0.5571	0.7018	0.8461	0.9909	4.5
-0.2887	-0.3394	-0.3898	-0.4409	-0.4923	-0.5434	-0.5948	-0.6459	-0.6971	-0.7487	-1.0086	-1.2704	-1.5313	-1.7932	4.6
0.1604	0.1885	0.2166	0.2450	0.2735	0.3019	0.3305	0.3589	0.3873	0.4160	0.5603	0.7058	0.8507	0.9962	4.7
-0.3145	-0.3694	-0.4242	-0.4795	-0.5351	-0.5902	-0.6458	-0.7012	-0.7565	-0.8120	-1.0913	-1.3736	-1.6546	-1.9366	4.8
0.1656	0.1944	0.2232	0.2524	0.2816	0.3106	0.3399	0.3691	0.3981	0.4274	0.5744	0.7229	0.8708	1.0193	4.9
-0.3418	-0.4010	-0.4607	-0.5206	-0.5801	-0.6399	-0.6996	-0.7593	-0.8194	-0.8795	-1.1795	-1.4819	-1.7855	-2.0888	5.0
0.1709	0.2005	0.2304	0.2603	0.2901	0.3199	0.3498	0.3796	0.4097	0.4397	0.5897	0.7409	0.8928	1.0444	∞

*imaginary* values of  $f_0$ ; it has only been possible to plot them on Fig. 1 because they happen to correspond to zero values of  $f_0$ . They have been placed on Fig. 1 because they represent the only solutions which are currently available for *imaginary* values of the variables; provision of a separate diagram for them therefore seemed extravagant. Clearly there is a great need for more study of the solutions with imaginary  $f_0$ .

### 3. INTERPOLATED SOLUTIONS

#### 3.1. Procedure

*Choice of co-ordinate system for interpolation.* The purpose of our study of the exact solutions of equation (1) is to obtain the functions needed in employing the calculation method of Paper 1. The functions required are  $F_2$ ,  $H_{24}$ , and to a lesser extent  $H_{12}$ , each expressed as functions of  $(\delta_2^2/\nu) du_G/dx$  and of  $v_S \delta_2/\nu$ .

It is noticeable from the preceding tables that the thickness ratios  $H_{12}$  and  $H_{24}$  vary relatively little, at least when conditions are far from those leading to separation. For this reason the interpolation was carried out on graphs having the  $H$ 's in the ordinate scales. Specifically, the data contained in the foregoing tables were plotted on two large-scale graphs, one having  $1/H_{12}$  and the other having  $H_{24}$  as ordinate; each graph had  $v_S \delta_2/\nu$ , as abscissa and  $\beta$  as parameter. Smooth curves for constant  $\beta$  were drawn through the points where possible. By interpolation along lines of constant  $v_S \delta_2/\nu$ , new curves of constant  $\beta$  were generated. Figs. 2 and 3 represent small-scale versions of the result.

The resulting tables of  $H_{12}$  and  $H_{24}$  were used for generating the other functions of interest by way of the relations which will now be introduced.

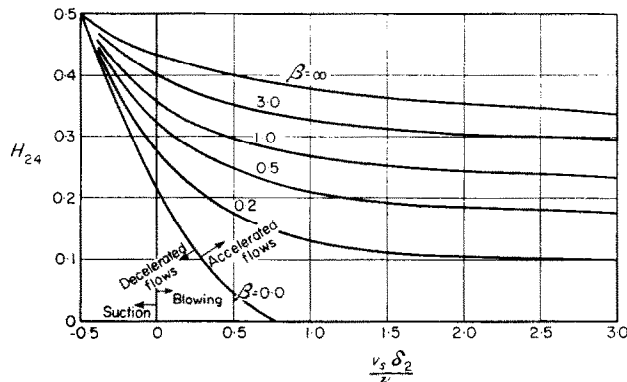


FIG. 2. Small-scale plot of  $H_{24}$  versus  $v_S \delta_2/\nu$  for a few  $\beta$ ; values obtained by interpolation.

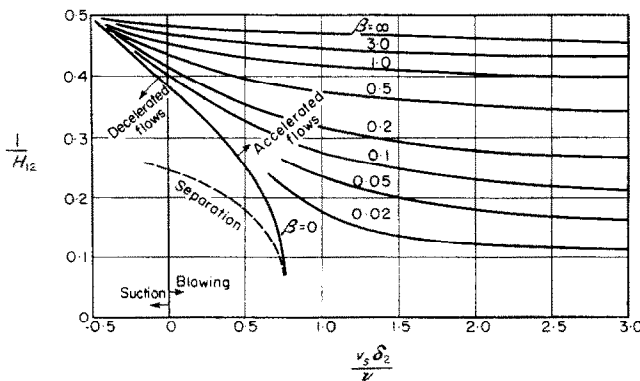


FIG. 3. Small-scale plot of  $1/H_{12}$  versus  $v_S \delta_2/\nu$  for a few  $\beta$ ; values obtained by interpolation.

*Derivation of  $F_2$  and  $(\delta_2^2/\nu) du_G/dx$ .* By integrating equation (1) over the range  $0 \leq \eta < \infty$  and replacing the value of  $f$  at infinity by

$$f_0 + \int_0^\infty \left( \frac{df}{d\eta} \right) d\eta$$

we obtain:

$$-f_0'' + f_0 + (1 - \beta) \int_0^\infty \frac{df}{d\eta} \left( 1 - \frac{df}{d\eta} \right) d\eta + \beta \int_0^\infty \left( 1 - \frac{df}{d\eta} \right) d\eta = 0 \quad (19)$$

wherein the terms in the quadratures have been grouped so as to correspond with those of equations (4), (6), etc. This equation corresponds to the integral momentum equation.

After multiplication of each term of equation (19) by  $\int_0^\infty (1 - df/d\eta) (df/d\eta) d\eta$  followed by direct substitution from equations (7), (8), (4), and (6), there results:

$$-H_{24} - \frac{v_S \delta_2}{\nu} + \frac{1 + \beta}{\beta} \frac{\delta_2^2}{\nu} \frac{du_G}{dx} + H_{12} \frac{\delta_2^2}{\nu} \frac{du_G}{dx} = 0 \quad (20)$$

which may be rewritten:

$$\frac{\delta_2^2}{\nu} \frac{du_G}{dx} = \frac{H_{24} + v_S \delta_2/\nu}{1 + (1/\beta) + H_{12}} \quad (21)$$

Substitution from equation (5) now leads to:

$$F_2 = 2 \left( \frac{1}{\beta} - 1 \right) \frac{H_{24} + v_S \delta_2/\nu}{1 + (1/\beta) + H_{12}} \quad (22)$$

Equations (21) and (22) connect the two quantities which remain to be evaluated with the quantities which are established by the interpolation procedure just described. They may therefore be used for the generation of tables. This has been done with the results described below.

*Derivation of values of  $f_0''$  and  $f_0$ .* The quantities  $f_0''$  and  $f_0$ , representing respectively the dimensionless shear stress and stream function at the phase boundary, may finally be derived from the quantities just mentioned by means of the following equations, which are deducible

from equations (4) to (8):

$$f_0'' = H_{24} \sqrt{[2(1 - \beta)/F_2]} \quad (23)$$

and

$$f_0 = - (v_S \delta_2/\nu) \sqrt{[2(1 - \beta)/F_2]}. \quad (24)$$

### 3.2. Presentation of tables

Table 7 contains the values of  $H_{12}$  and  $H_{24}$  obtained by the above interpolation procedure. The arguments are  $v_S \delta_2/\nu$  and  $\beta$ . Both positive and negative values of each of these quantities are given, although positive values of  $\beta$  predominate. The range of arguments considered was restricted by the existence of exact or asymptotic solutions between which to interpolate. Within this range, we have attempted to give sufficient values to permit rapid interpolation (in  $1/\beta$ , if not in  $\beta$ ).

Table 8 contains the corresponding values of the quantities  $F_2$  and  $(\delta_2^2/\nu) du_G/dx$ , arranged in a similar fashion.

### 3.3. Presentation of graphs

To permit rapid use of the data contained in the tables, and in order to permit the nature of the functions to be seen clearly, the data have been displayed graphically in Figs. 4 and 5.

The first of these, which is in two parts, presents the quantity  $H_{24}$  plotted against  $(\delta_2^2/\nu) du_G/dx$ , for various values of the parameter  $v_S \delta_2/\nu$ . Fig. 4(a) gives the data for large positive values of this parameter; Fig. 4(b) gives the data for negative and small positive values of the parameter. Also plotted as points are the exact solutions referred to earlier, with the corresponding  $v_S \delta_2/\nu$  values by their sides. Comparison of the location of the points with respect to the lines permits the success of the interpolation procedure to be gauged.

Figure 5, which is in three parts, provides curves of  $F_2$  versus  $(\delta_2^2/\nu) du_G/dx$  for various values of  $v_S \delta_2/\nu$ . Once again the exact solutions appear as points.

We shall not discuss the reasons for the shapes of the curves displayed, since this would fit more properly into a comprehensive discussion of the mathematics of equation (1). We merely note in passing that the two points with  $\beta = -1$  and  $\beta = -4$  for  $f_0 = 0$  fit neatly on to the prolongations of the lines for  $f_0 = 0$  with  $\beta = 0$ , and lie

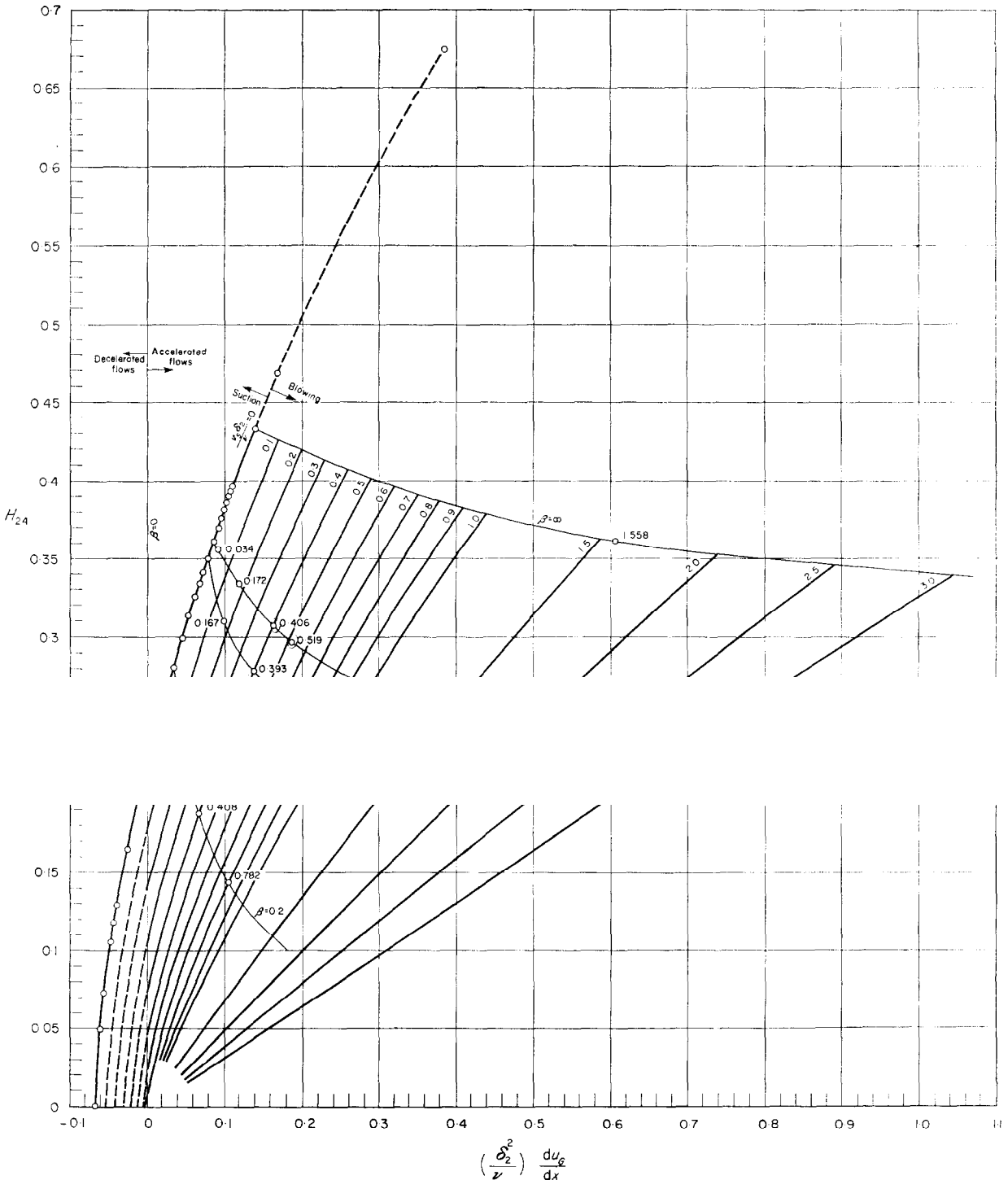


FIG. 4(a). Blowing.  $H_{24}$  as a function of  $(\delta_2^0/\nu) du_G/dx$ ; blowing parameter  $v_S \delta_2/\nu$ ;  $\circ$ : exact solutions, adjacent number indicating  $\beta$ -value; those on line  $(v_S \delta_2/\nu) = 0$  come from Table 1; others come from Table 3; those on line  $(\delta_2^0/\nu) (du_G/dx) = 0$  have been omitted for clarity; ----: uncertain accuracy.



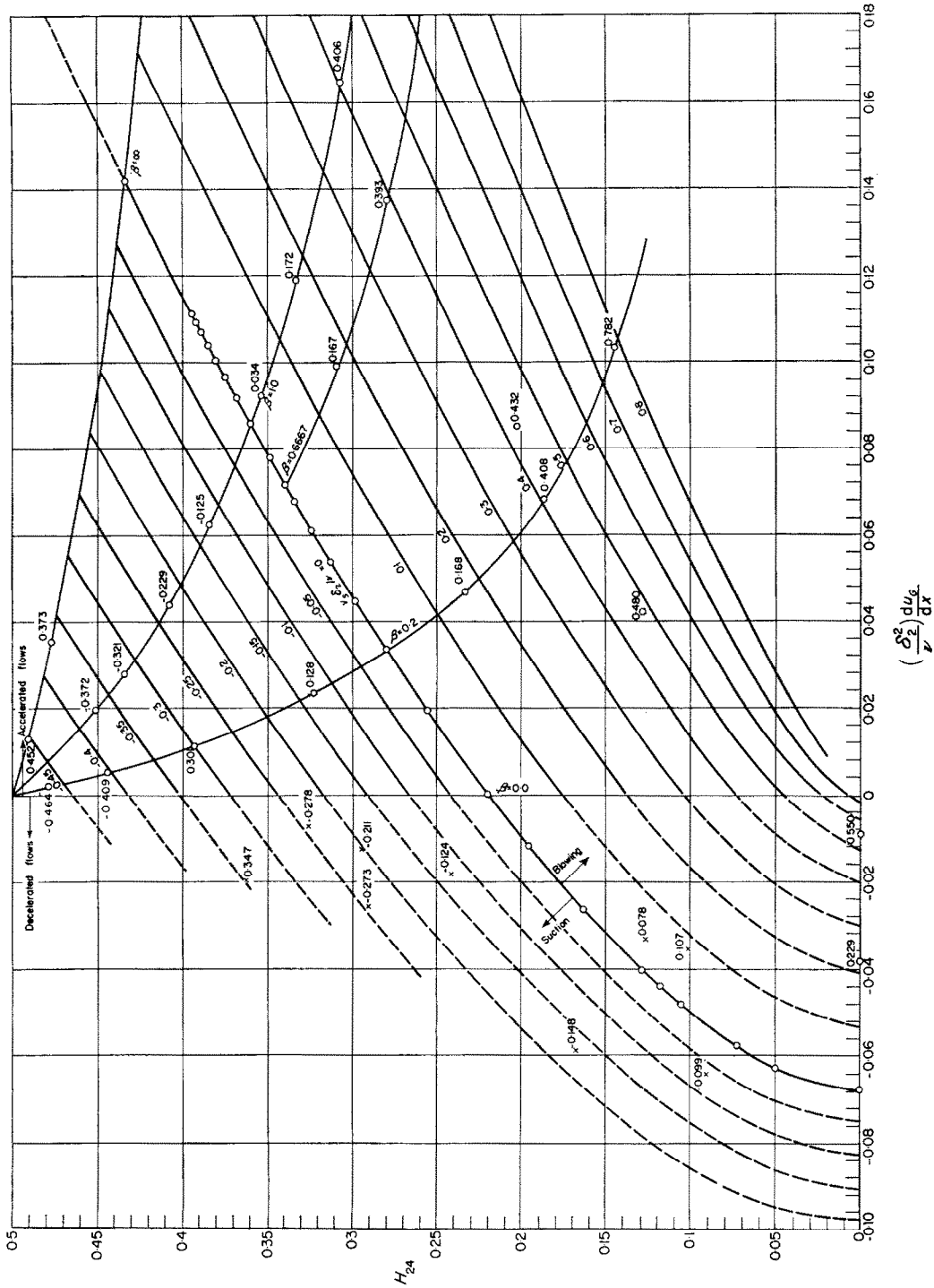


FIG. 4(b). Suction and slight blowing.  $H_{24}$  as a function of  $(\delta_2^2/\nu) dU_e/dx$ ; Suction and blowing parameter  $v_x \delta_2 / \nu$ ; ○ : exact solutions, adjacent numbers indicating values of  $v_x \delta_2 / \nu$ ; × : exact solutions of doubtful accuracy those on line  $v_x \delta_2 / \nu = 0$  come from Table 1; others come from Table 3; those on line  $(\delta_2^2/\nu) (dU_e/dx) = 0$  have been omitted for clarity; - - - - : uncertain accuracy.

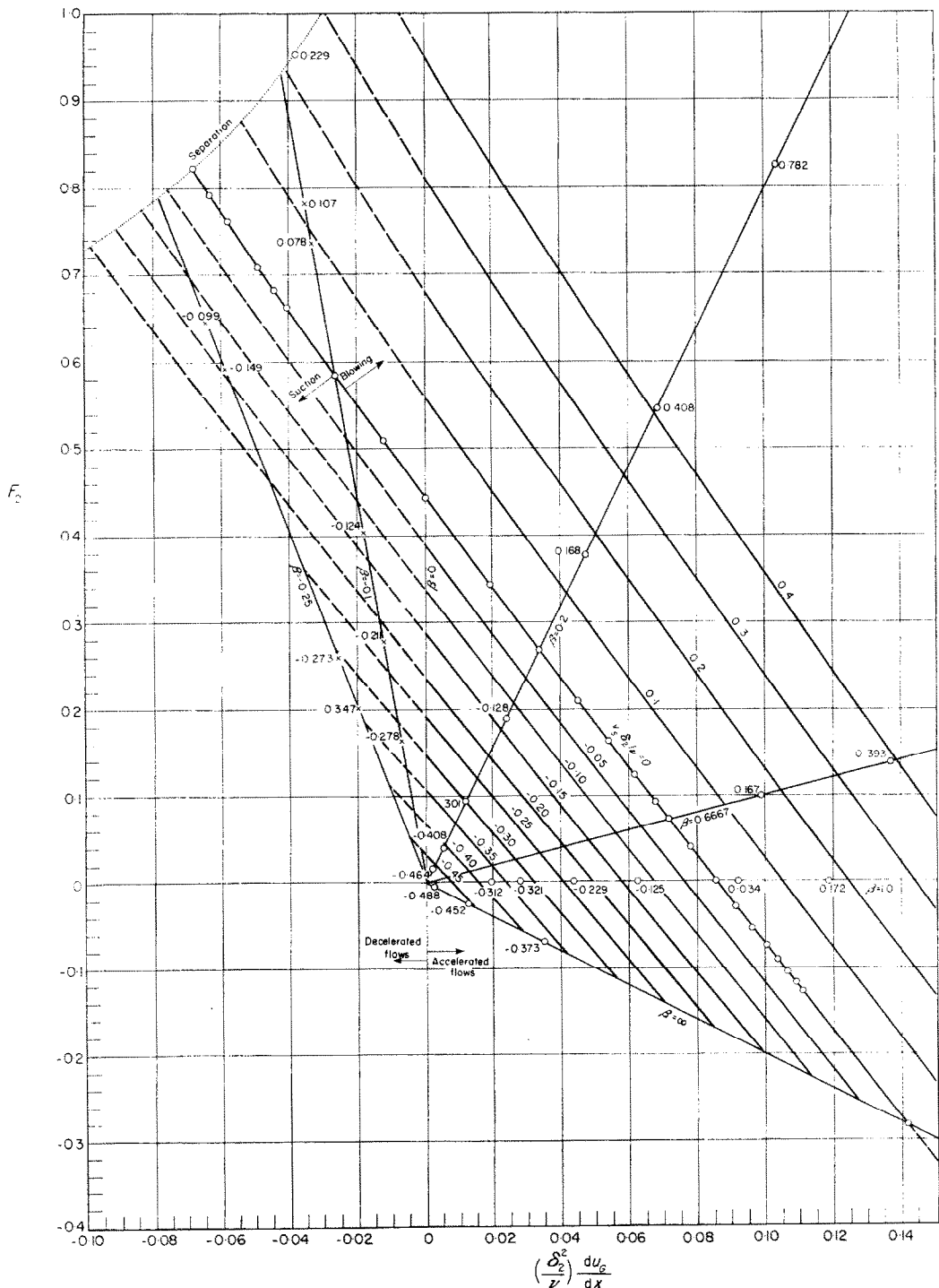


FIG. 5(a). Suction and weak blowing.  $F_2$  as a function of  $(\delta_2^2/v) du_G/dx$ ; suction or blowing parameter  $v_S \delta_2/v$ ;  $\circ$ : exact solutions, adjacent numbers indicating values of  $v_S \delta_2/v$ ; those on line  $(v_S \delta_2/v) = 0$  come from Table 1; others come from Table 3; those on line  $(\delta_2^2/v) (du_G/dx) = 0$  have been omitted for clarity; - - - : uncertain accuracy.

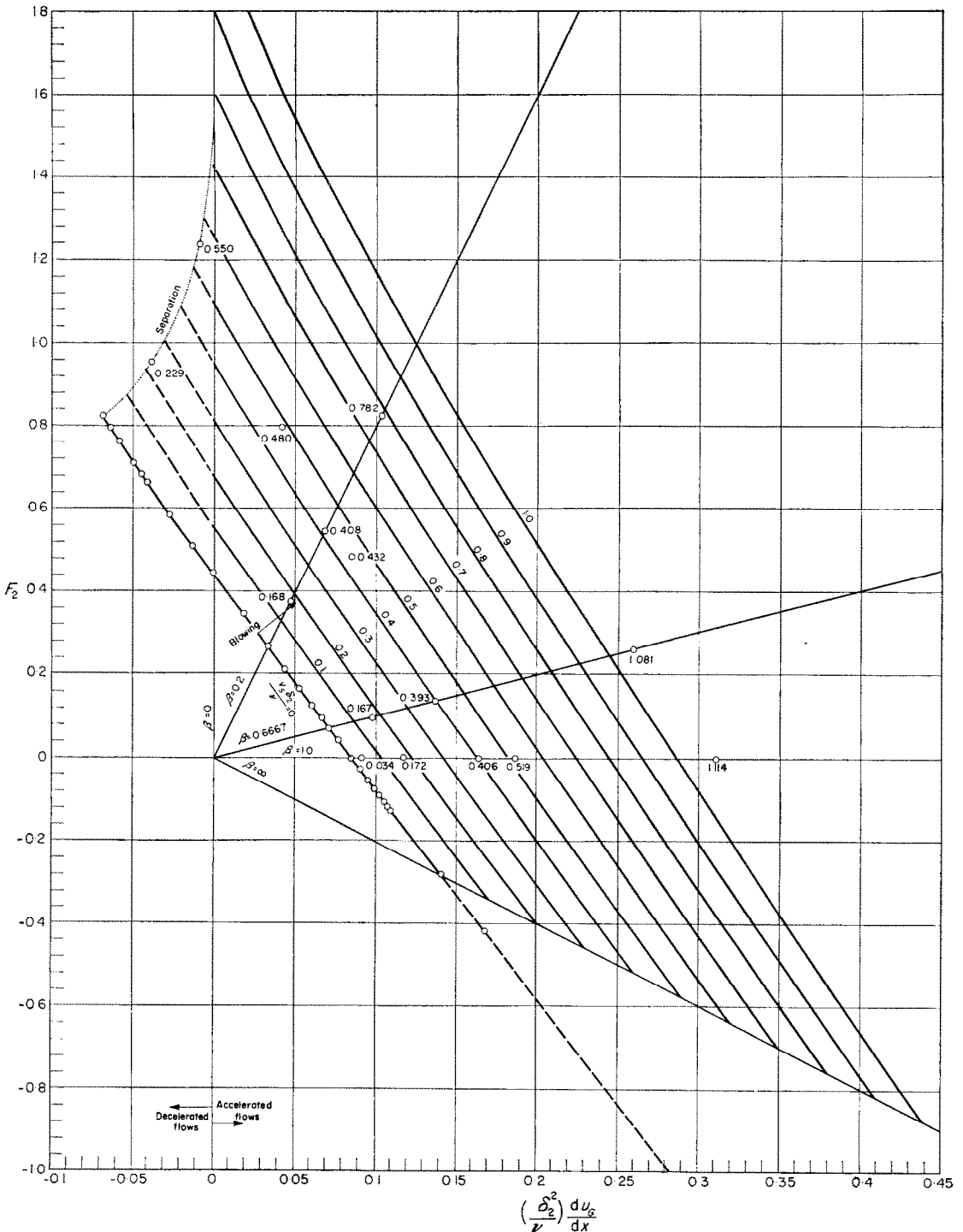


FIG. 5(b). Moderate blowing.  $F_2$  as a function  $(\delta_2^2/\nu) du_c/dx$ ; blowing parameter  $v_S \delta_2/\nu$ ;  $\circ$ : exact solutions, adjacent numbers indicating values of  $v_S \delta_2/\nu$ ; those on line  $(v_S \delta_2/\nu) = 0$  come from Table 1; others come from Table 3; those on line  $(\delta_2^2/\nu) (du_c/dx) = 0$  have been omitted for clarity; ----: uncertain accuracy.

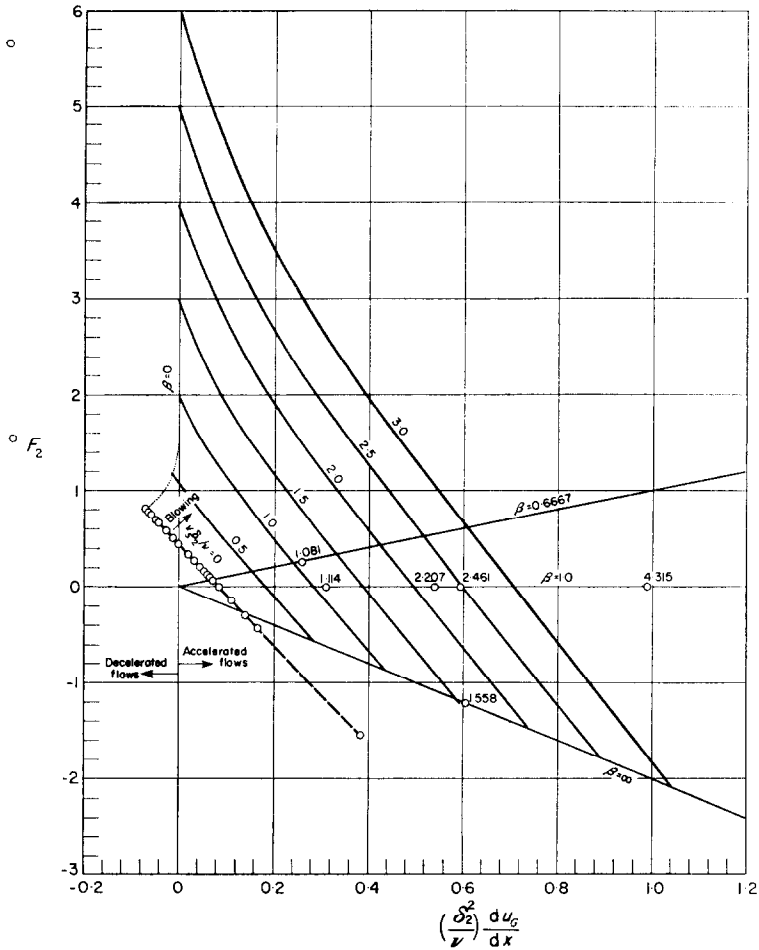


FIG. 5(c). Intensive blowing.  $F_2$  as a function of  $(\delta_2^2/\nu) du_G/dx$ ; blowing parameter  $v_S \delta_2/\nu$ ;  $\circ$ : exact solutions adjacent numbers indicating values of  $v_S \delta_2/\nu$ ; those on line  $(v_S \delta_2/\nu) = 0$  come from Table 1; others come from Table 3; those on line  $(\delta_2^2/\nu) (du_G/dx) = 0$  have been omitted for greater clarity.

positive. This means that they correspond to accelerated boundary layers; for  $\delta_2^2$  is essentially positive, so  $u_G$  must be locally increasing with  $x$ . These are the points with the imaginary  $f_0''$ , it will be remembered.

*The role of  $\beta$ .* In this connexion it is interesting to reflect that the often-repeated statement that  $\beta > 0$  corresponds to accelerated flows, while  $\beta < 0$  corresponds to decelerated flows, is only partially true. Another aspect of the situation can be recognized by inspecting Fig. 5(a), for example. On such a diagram, equation (5)

ensures that all points with a given  $\beta$  lie on a line through the origin, of slope  $2(1/\beta) - 1$ ; the line for  $\beta = \infty$ , for example, has slope  $-2$ .

Now the lines for constant  $v_S \delta_2/\nu$  are very nearly straight and parallel; close to the origin their slope\* must be  $-8$ . Moreover they all lie on one side of the origin. It follows that, whenever,

$$+\infty > 2 \left\{ \frac{1}{\beta} - 1 \right\} > -8 \quad (25)$$

\* See Appendix A for proof.

solutions, i.e. the intersections of the constant- $\beta$  lines with the lines of constant  $v_S \delta_2 / \nu$ , lie in the region where  $(\delta_2^2 / \nu) du_G / dx$  is positive. When the directions of the inequalities are reversed, the solutions lie in the left-hand half of the diagram. Consequently the flow is accelerated whenever, for small  $v_S \delta_2 / \nu$ ,

$$\beta > 0, \text{ or } \beta < -0.333. \quad (26)$$

This is not to say that, for  $\beta = -0.4$  for example, no solution can be found which corresponds to decelerated flow; for this to happen the line for constant  $v_S \delta_2 / \nu$  would have to sag downward on the left so that the  $\beta = -0.4$  line could intersect it there.

*Graphical representation of "real and imaginary domains".* The opportunity will be taken to point out the regions on plots with the co-ordinates of Fig. 5 which correspond to real values of  $f$  and  $\eta$ , and those which correspond to imaginary ones. This will be explained by reference to Fig. 6, which shows lines of constant  $\beta$  shown on the  $F_2$  versus  $(\delta_2^2 / \nu) du_G / dx$  plane. [Unlike Fig. 5,

Fig. 6 has the same scale for both ordinate and abscissa.]

A brief examination leads to the following conclusions:

- (i)  $f$  and  $\eta$  are real whenever  $\beta$  and  $du_G / dx$  have the same sign. This occurs to the right of the line for  $\beta = \pm \infty$ .
- (ii) To the left of this line  $f$  and  $\eta$  must be imaginary.
- (iii) Each line of constant  $\beta$  (except that for  $\beta = \pm \infty$ ) extends into the "real domain" on one side of the origin and the "imaginary domain" on the other.

It should be clearly understood that the fact that a solution lies in the region just designated "imaginary domain" in no way signifies that it is without physical significance; for though  $f_0$  and  $\eta$  may be imaginary, quantities such as  $v_S \delta_2 / \nu$ ,  $F_2$ , etc. are all real.

The integration of equation (1) for imaginary values of  $f$  and  $\eta$  may appear to be a mysterious operation. All that is necessary however is to define new variables, say:

$$\phi \equiv f\sqrt{-1} \quad (27)$$

and

$$\chi \equiv \eta\sqrt{-1}. \quad (28)$$

Equation (1) therefore becomes:

$$\frac{d^3 \phi}{d\chi^3} - \frac{\phi d^2 \phi}{d\chi^2} - \beta \left\{ 1 - \left( \frac{d\phi}{d\chi} \right)^2 \right\} = 0 \quad (1a)$$

and the boundary conditions (2) become

$$\left. \begin{aligned} \chi = 0: & \quad \frac{d\phi}{d\chi} = 0, & \quad \phi = f_0\sqrt{-1} \\ \chi = \infty: & \quad \frac{d\phi}{d\chi} = 1 \end{aligned} \right\} \quad (2a)$$

Now all the quantities in the problem have real values, and solution may proceed in a straightforward manner.

### 3.4. Accuracy

It is believed that, over most of the range covered by the tables, the accuracy in the values of  $H_{12}$  and  $H_{24}$  is better than  $\pm 0.3$  per cent. This may not have been achieved for the smaller

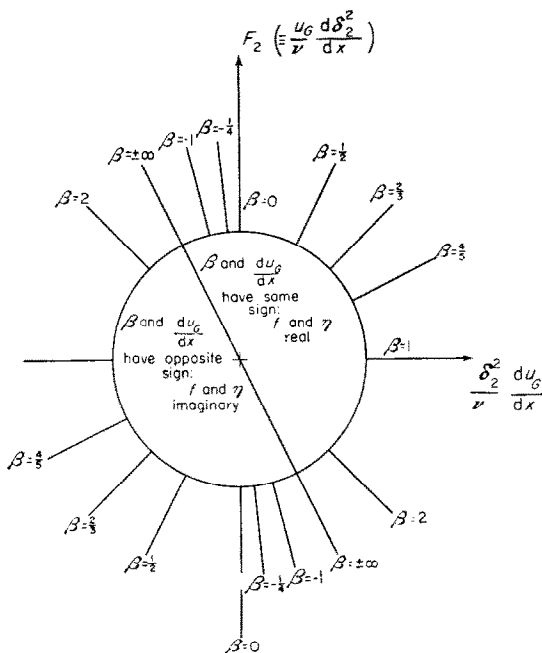


FIG. 6. Illustrating on a diagram of  $F_2$  versus  $(\delta_2^2 / \nu) du_G / dx$  the region for which  $f$  and  $\eta$  have real values and that where they have imaginary values.

values of  $\beta$ , however, nor for the larger values of  $v_S \delta_2 / \nu$ .

A check on the overall accuracy was afforded by calculating values of  $f_0''$  and  $f_0'$  from the tables, by way of equations (23) and (24), for the values of  $\beta$  considered by Bain [16]; Bain's results had not been used in the construction of the tables because of their incompleteness. When the resultant values were plotted as curves of  $f_0''$  versus  $f_0'$  for fixed  $\beta$ , the curves through them were undistinguishable from those through Bain's points.

### 3.5. Use of the tables

The method of use of Tables 7 and 8 and of Figs. 4 and 5 have been explained thoroughly in Paper 1 of this series (Spalding [1]). No attempt will be made to discuss the matter further here.

## 4. CONCLUSIONS

- (i) A large number of solutions have been found to the equation governing the velocity distribution in a "similar" laminar uniform-property boundary layer in the presence of pressure gradient and mass transfer through the wall.
- (ii) Interpolation means have been found, permitting the construction of charts and tables containing those properties of the "similar" solutions which are useful in solving "non-similar" boundary-layer problems by the method of Paper 1 of this series.
- (iii) The charts and tables are not as extensive as is necessary for the solution of all practical problems. More solutions of the differential equation must be established before this restriction can be removed. This is particularly true of the solutions for imaginary values of the non-dimensional stream-function  $f_0$ .
- (iv) It has been established that solutions of equation (1) for imaginary values of the variables not only have physical significance but merge smoothly into those with real values of the variables, when plotted in terms of the quantities  $v_S \delta_2 / \nu$ ,  $F_2$ , etc.

## 5. APPEAL

The authors are well aware that they may have missed some relevant publications, particularly those published in languages other than English and German. They would like to learn of any exact solutions of the equation which have been omitted, and would especially welcome complete tables of relevant numerical data. If sufficient data are forthcoming, they will publish amended or extended versions of the tables of functions contained in the present report.

The authors would also be glad to learn of any programme for computing new solutions to equation (1) and the relevant boundary conditions, particularly those for imaginary values of  $f_0$ .

## ACKNOWLEDGEMENTS

This paper is based on part of the London University Ph.D. thesis of one of the authors (H.L.E.), who wishes to thank CSIRO, Australia, for the grant of leave, and of an overseas studentship, which made the work possible. Thanks are also due to Mr. R. W. Bain, National Engineering Laboratory, Scotland, for permission to cite the results contained in Table 5, and to Miss M. P. Steele for assistance with the preparation of the manuscript.

The work was carried out under the terms of a contract between the National Engineering Laboratory and the Imperial College. Permission for publication has been given by the Director of the N.E.L.

## REFERENCES

1. D. B. SPALDING, Mass transfer through laminar boundary layers—1. The velocity boundary layer. *Int. J. Heat Mass Transfer*, **2**, 15 (1961).
2. V. M. FALKNER, A further investigation of the boundary-layer equations. *Brit. Aero. Res. Council R and M* 1884 (1937).
3. V. M. FALKNER, Simplified calculation of the laminar boundary layer. *Brit. Aero. Res. Council R and M* 1895 (1941).
4. W. MANGLER, Boundary layers. 1.2 Special exact solutions. *AVA Monograph, Reports and Translations No. 1001*. (Edited by W. TOLLMIE.) (1948).
5. H. HOLSTEIN, Similar boundary layers at permeable walls. *Deutsche Luftfahrtforschung U.M.* 3050 (1943).
6. D. R. HARTREE, On an equation occurring in Falkner and Skan's approximate treatment of the equations of the boundary layer. *Proc. Camb. Phil. Soc.* **33**, 223–239 (1937).
7. H. W. EMMONS and D. LEIGH, Tabulation of the Blasius function with blowing and suction. *Harvard Univ. Comb. Aero. Lab., Interim Technical Report No. 9* (1953).

8. W. MANGLER, Laminare Grenzschicht mit Absaugung und Ausblasen. *Deutsche Luftfahrtforschung U.M.* 3087 (1944).
9. W. B. BROWN and P. L. DONOUGHE, Tables of exact laminar boundary-layer solutions when the wall is porous and fluid properties are variable. NACA TN 2479 (1951).
10. H. SCHAEFER, Laminare Grenzschicht zur Potentialströmung  $u = u_1 x^m$  mit Absaugung und Ausblasen. *Deutsche Luftfahrtforschung U.M.* 2043 (1944).
11. E. R. G. ECKERT, P. L. DONOUGHE and B. J. MOORE, Velocity and friction characteristics of laminar viscous boundary layer and channel flow with ejection or suction. NACA TN 4102 (1957).
12. P. L. DONOUGHE and J. N. B. LIVINGOOD, Exact solutions of laminar boundary-layer equations with constant property values for porous wall with variable temperature. NACA TN 5151. Superseded by TR 1229 (1954).
13. H. SCHLICHTING and K. BUSSMANN, Exakte Lösungen für die laminare Reibungsschicht mit Absaugung und Ausblasung. *Schrift. d. D. Akad. Luftfahrtforschung* 7 B, Heft 2 (1943).
14. J. PRETSCH, Laminar boundary layer with intense suction and blowing. *Deutsche Luftfahrtforschung U.M.* 3091 (1944).
15. E. J. WATSON, The asymptotic theory of boundary layer flow with suction. *Brit. Aero. Res. Council R and M* 2619 (1952).
16. R. W. BAIN, Unpublished work at National Engineering Laboratory (1959).

APPENDIX A

*Relation between  $F_2$  and  $(\delta_2^2/\nu) du_G/dx$  when  $v_S \delta_2/\nu$  is close to  $-0.5$*

Inspection of Figs. 2 and 3 shows that, for all values of  $\beta$ ,  $H_{24}$  tends to 0.5 and  $H_{12}$  tends to 2.0 as  $v_S \delta_2/\nu$  tends to  $-0.5$ . This is the case of intense suction, for which the velocity distribution takes up an exponential form.

Substitution of these values in equations (21) and (22), followed by elimination of  $\beta$  between them leads to the equation:

$$F_2 + 8 \frac{\delta_2^2}{\nu} \frac{du_G}{dx} = 1 + 2 v_S \delta_2/\nu. \quad (A1)$$

For fixed  $v_S \delta_2/\nu$ , this is a line with slope  $-8$ .